Dynamics of Thioether Molecular Rotors: Effects of Surface Interactions and Chain Flexibility

Heather L. Tierney, Ashleigh E. Baber, and E. Charles H. Sykes

Department of Chemistry, Tufts University, Medford, Massachusetts 02155-5813

Alexey Akimov and Anatoly B. Kolomeisky*

Department of Chemistry, Rice University, Houston, Texas 77005-1892

Received: February 26, 2009; Revised Manuscript Received: March 31, 2009

Recent single-molecule experiments indicated that thioethers (dialkyl sulfides) on gold surfaces act as thermally- or mechanically activated molecular rotors, although the mechanisms for these phenomena are not yet clearly understood. Here we present theoretical and experimental investigations of the rotational dynamics of these thioether molecules. Single-molecule studies utilizing low-temperature scanning tunneling microscopy allowed us to determine rotational rates and activation energies for the rotation of symmetric dialkyl sulfides. It was found that the rotational energy barriers increased as a function of alkyl chain length but then quickly saturated. Molecular dynamics simulations have also been performed in order to understand the molecular rotations of thioethers, and our theoretical calculations agree well with experimental observations. It is argued that the observed rotational dynamics of dialkyl sulfides are determined by the effective interactions with the surface and the flexibility of the alkyl chains. These results suggest possible ways to control and utilize thioether rotors at the single-molecule level.

1. Introduction

Molecular machines driven by chemical, light, or thermal energies are pervasive in nature.[1−5] They play important roles in different biological processes including cellular transport, cell division, muscle contraction, genetic transcription, and translation.[1−3] These biological motors are highly efficient, versatile, and robust nanomachines that have stimulated significant efforts in creating analogous nanoscale artificial devices.[6,7] However, applications for these manmade molecular motors are still almost nonexistent in current technology. This is because the most fundamental problem of how energy is transformed into mechanical motion is still not well understood at the nanoscale.[3,4]

One important class of nanomachines is molecular rotors. Most studies of rotors at the nanoscale involve complex organic molecules in solution.[7−11] However, many potential applications of molecular rotors in nanotechnology would require their association with surfaces. It is much easier to monitor and control surface-bound molecular rotors, as fixing their positions in two dimensions allows for more facile coupling to other nanomechanical devices. Surface-mounted rotations of small molecules, such as PF_3[12] and O_2,[13] as well as large organic molecules[14−18] have been reported. A lot of attention has also been devoted to investigating rotational dynamics of porphyrins.[19−25] Using scanning tunneling microscopy (STM) rotational rates and energy barriers have been determined. A related technique of inelastic electron tunneling (IET) has been used to probe rotations of acetylene[26−28] and *cis*-2-butene molecules.[29,30] Rotational dynamics of chloromethyl- and dichloromethylsilyl molecules on fused silica surfaces have been analyzed via STM and by measuring dielectric responses.[31−34] Experiments also show that halogenated thiophenol molecules can rotate on Cu{111} surfaces even at low temperatures.[35,36]

Experimental achievements in development and analysis of molecular rotor systems have stimulated theoretical efforts to understand rotational dynamics.[37−40] Michl and Horinek[37,38] investigated motions of altitudinal molecular rotors using molecular dynamics (MD) computer simulations based on the universal force field (UFF) and taking into account electronic friction on the surface. Theoretical computations have suggested that there are several dynamic regimes of rotation. A different approach has been applied in refs 39 and 40 where rotational barriers have been calculated by utilizing quantum-chemical density-functional methods. Although theoretical studies have helped to explain some of the experimental observations, they were not able to explain the mechanisms of rotational dynamics on surfaces.

Recently a new, stable and robust system of molecular rotors, which consists of thioether molecules bound to gold surfaces, has been introduced.[41] In this system, the molecular rotation could be controlled either thermally or mechanically. STM has been used to obtain the rotational properties of thioether molecules at different temperatures. Experiments showed that dimethyl sulfide had low activation energy for its rotation, while all other investigated dialkyl sulfides (with longer chains) had similar rotational barriers. This result was rather surprising since one could argue that longer alkyl chains should interact stronger with a gold surface, significantly slowing down the rotations of individual molecules. In this paper mechanisms for the rotation of thioethers on Au have been investigated by utilizing a comprehensive approach that combines both experimental and theoretical methods.

2. Experimental Studies

All STM experiments were performed in a low-temperature, ultrahigh vacuum (LT-UHV) microscope built by Omicron Nanotechnology. The Au(111) sample was purchased from

* To whom correspondence should be addressed. E-mail: tolya@rice.edu.

10.1021/jp9017844 CCC: $40.75
Published on Web 04/24/2009

MaTecK and was prepared by cycles of Ar sputtering (1.0 keV/10 μA) for 30 min followed by 2 min anneal periods up to 760 K. Approximately 12 of these sputter/anneal cycles were performed upon receiving the crystal, followed by a further 2 sputter/anneal cycles between each STM experiment. After the final anneal, the crystal was transferred in less than 5 min into vacuum ($<5 \times 10^{-10}$ mbar) to the precooled STM. In approximately 30 min, the sample cooled from room temperature to either 78 or 7 K. All images were recorded with etched W or cut Pt/Ir tips, and voltages refer to the sample bias. Thioethers (between 99.9 and 99.95% purity) were obtained from Sigma Aldrich and were further purified by cycles of freeze/pump/thaw prior to introduction to the STM chamber via a leak valve. The molecules were deposited onto the sample by a collimated molecular doser while the tip was scanning. The STM stage was equipped with a sample heater capable of controllably heating the sample and tip up to 50 K above the base temperature.

3. Theoretical Computations

To understand the mechanisms of molecular rotation for thioethers on gold surfaces, MD computer simulations were performed that utilized a recently developed method for the analysis of thermally induced motions of nanocar molecules.[42] This method is based on rigid-body MD calculations that utilize the UFF. The advantage of this approach for analyzing the rotational dynamics of thioethers is that almost all atomic interactions are explicitly taken into account while some of the internal degrees of freedom are neglected. This allows the calculations to be sped up significantly, yielding longer trajectories, and providing a better description of dynamic properties.[42]

3.1. Calculation Details. Rigid-body MD calculations were performed in order to study the rotational dynamics of a series of symmetric dialkyl sulfides $[CH_3(CH_2)_n-S-(CH_2)_nCH_3]$ with $n = 0, 1, 2, 3$. For simplicity, these molecules were labeled as C_{n+1}, which corresponds to the number of carbon atoms in each alkyl chain. Before simulations were performed, all initial structures were optimized such that they were always started from states close to equilibrium. For each molecule and each of the 5 temperatures used (25, 35, 50, 78, and 100 K), 10 trajectories were obtained. To maintain a constant temperature in the simulations, a Nose−Poincare thermostat[43] with the symplectic integrator for rigid-body MD was utilized.[44] All trajectories were 2.5−5 ns long since a variable time-step approach was used. The UFF[45] was employed to describe intramolecular interactions in thioethers and some interactions between the surface and the molecules under consideration. To describe chemisorption of the sulfur atom, a Morse-type binding term was chosen. All parameters for the intramolecular interactions were calculated on the basis of the UFF rules. The parameters of the Morse-type binding functional were adopted from different sources[45,46] and were subject to variation.

The surface potential was constructed in the following way. For each atom in the thioether molecule, its coordinates were projected onto the surface plane and a lattice cell was reconstructed around the projection of the atoms in the thioether. This cell was represented by four explicit atoms in a fcc(111) coordination (parallelogram). The rest of the surface potential was modeled by constructing the explicit surface potential via replicas of this minimal lattice cell. Usually $N = 5$ lattice cells were used on each side of the initial central cell around the projection. Therefore, for each atom of the molecule under consideration $4(N + 1)^2 = 144$ atoms of the surface were used explicitly. Thus, the size of the surface slab was $b(2N + 1) = 31.66$ Å, where b is the lattice size of the (111) surface. Bonded surface-molecule interactions have also been modeled explicitly. The same projection approach has been used for bonded surface-molecule interactions, but with Morse potentials instead of Lennard-Jones potentials. To avoid discontinuity in the potential that could lead to anomalous diffusive behavior and could bias results, the following switching function was used

$$SW(R, R_{on}, R_{off}) = \begin{cases} 1, R < R_{on} \\ \left(\frac{R_{off} - R}{R_{off} - R_{on}}\right)^3\left[1 + 3\left(\frac{R - R_{on}}{R_{off} - R_{on}}\right) + 6\left(\frac{R - R_{on}}{R_{off} - R_{on}}\right)^2\right], \\ 0, R > R_{off} \end{cases}$$
$$R_{on} \le R \le R_{off} \quad (1)$$

Parameters for the switching function were chosen to be $R_{on} = 2\sqrt{3}b$ and $R_{off} = 5b$, where $b = a/\sqrt{2}$ and is the lattice size of (111) surfaces. In addition, charges for each molecule were computed before each simulation using a charge equilibration scheme for molecular dynamics.[45]

In the experimental studies, a Au(111) surface was used, which reconstructs into three different domains.[47,48] Since the properties of the surface could be critical for rotational dynamics, MD simulations for C_1-C_6 molecular rotors (except C_5) were also performed on three different domains of the reconstructed gold surface. The gold surface was represented by three layers with a total number of atoms around 1150. In order to obey the periodicity of the reconstructed surface at least eleven shells (unit cells) had to be used in the direction of reconstruction, but typically sixteen shells were used to avoid discontinuities in the potential. Thus the size of the superlattice unit was 2.88 Å $\times$ 22 = 31.68 Å in the reconstruction direction and 2.88 Å in the perpendicular direction. The first layer was different, as it was contracted in one of the directions (the reconstructed direction) by a factor of (22/23).

Three different surface sites were considered, which corresponded to fcc, hcp, and sol (soliton) domains. This was done by putting the center of the molecule on each of these areas and then the energy was minimized. Simulations were performed starting in these three different areas and while some molecules diffused around the surface during simulations (especially at high temperatures), in most cases (especially at low temperatures) molecules were mostly immobile.

3.2. Analysis of the MD Trajectories. In the STM experiments, the rotational frequency of the molecules was measured by recording the switching events between three distinct orientations. Each orientation was associated with some average state of the tunneling current, and the rotational rate was measured as a frequency of changing between these orientations. In the MD simulations, a similar analysis has been done.

A vector

$$\vec{R}_{21} = \vec{R}(C_{\alpha,left}) - \vec{R}(C_{\alpha,right}) \quad (2)$$

was chosen to connect two α-carbons in each chain as a vector that determines the time-dependent orientation of the molecule. An angle, $\phi(t)$, was then defined as the angle between this time−dependent vector and some predefined fixed direction. This angle was assumed to be a variable describing the orientation of the molecule with respect to the surface. Since the angle is a continuous function, a threshold value for ϕ was also introduced to distinguish between the three discrete states, as was done experimentally.

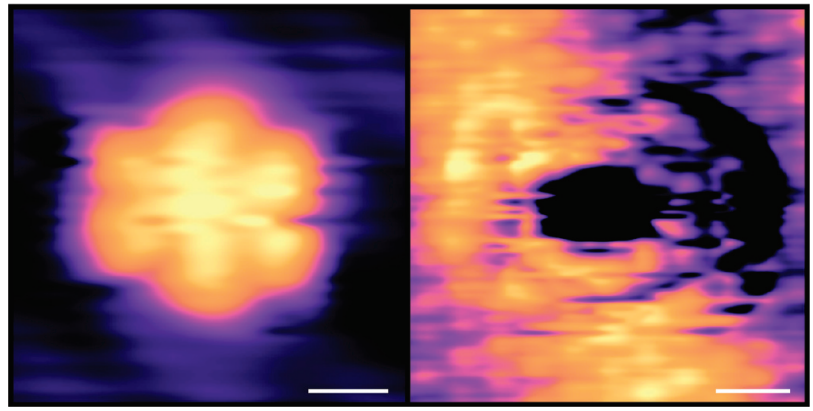

Figure 1. STM image of a single dibutyl sulfide (C_4) molecular rotor that appears as a hexagon when rotating on a time scale faster than that of STM imaging. (a) C_4 images as a hexagon with six distinct lobes due to its three nearly equivalent orientations with respect to the underlying Au lattice ($I = 0.1$ nA, $V_{tip} = 0.3$ V, 7 K). (b) Atomic resolution of the Au substrate resolved under a C_4 molecule helps assign the adsorption site of the molecule as near a 3-fold hollow site ($I = 0.5$ nA, $V_{tip} = -0.2$ V, 78 K). Scale bars = 0.5 nm.

4. Results and Discussion

Low-temperature STM revealed that individual thioether molecules adsorbed on Au(111) appeared as hexagons at a temperature of 78 K (see Figure 1). As the alkyl tails of the molecules rotated around the Au−S bond (axle), the rotors spent the majority of their time in three distinct orientations due to the 3-fold symmetry of the underlying Au(111) substrate. In Figure 1a, six lobes are clearly visible due to these three nearly equivalent orientations. If the lobes of the thioethers were labeled as the head or the tail, there are actually six possible orientations with respect to the surface, although only three states are distinguishable due to the symmetry of the molecules. Further imaging with atomic resolution (Figure 1b) showed the Au atoms resolved underneath the rotor molecule, which itself appeared as a depression in this image. Such high-resolution imaging in which the tip state allowed the atoms in the surface to be imaged permitted the adsorption site of dibutyl sulfide (C_4) to be assigned as near 3-fold hollow.

At a much lower temperature of 7 K, all of the thioether molecules appeared linear in shape, with the exception of dimethyl sulfide (C_1), which still looked hexagonal due to its low barrier to rotation. As the thioethers were heated, they began to spin and quickly appeared hexagonal on the time scale of STM imaging. For diethyl (C_2), dibutyl (C_4), and dihexyl (C_6) sulfide, the rotors began rotating at approximately the same temperature of 16 ± 2 K (see Figure 2). C_6 never imaged exceptionally well, probably due to the extra degrees of freedom from the length of the alkyl chains, but it too appeared roughly hexagonal at 16 K.

MD simulations provided trajectories for the motion of individual molecules from which the rotational dynamics of the thioethers could be analyzed. As shown in Figure 3, temperature strongly affected rotation. Similar to experimental observations, at low temperatures C_1 molecules already rotated quickly, while C_4 rotated very slowly (Figure 3a). This observation could be deduced from the fact that C_1 occupied all six possible orientations with almost equal probability (corresponding to the six lobes imaged in STM); however C_4 preferred only one configuration during the time of one MD simulation. This situation changed at higher temperatures (Figure 3b) where C_4 also started to rotate more quickly.

Because of the compression of the Au(111) surface, an intermediate state between the linear and hexagonal appearance was observed upon heating the thioethers rotors. Since the Au substrate is compressed in one direction (leading to the

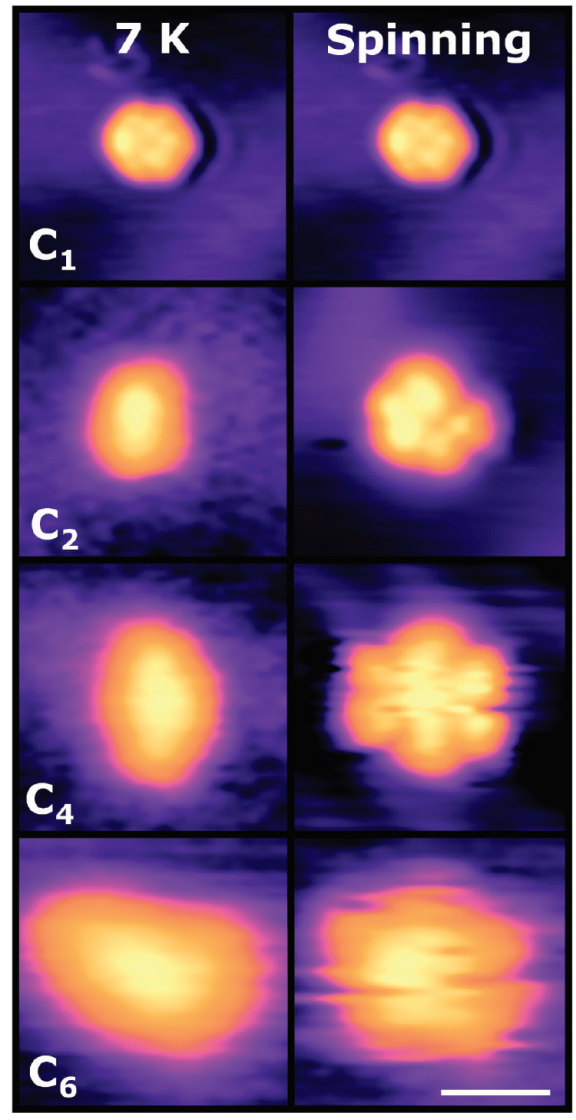

Figure 2. STM images reveal that dialkyl sulfide molecular rotors bound to Au(111) begin to rotate as the surface temperature is raised. Dimethyl (C_1), diethyl (C_2), dibutyl (C_4), and dihexyl (C_6) sulfide molecules are shown as linear vs hexagonal molecules at low and higher temperature, respectively, with the exception of C_1. C_1 has a low barrier to rotation and appears to be rotating even at a temperature of 7 K. Scale bar = 1 nm.

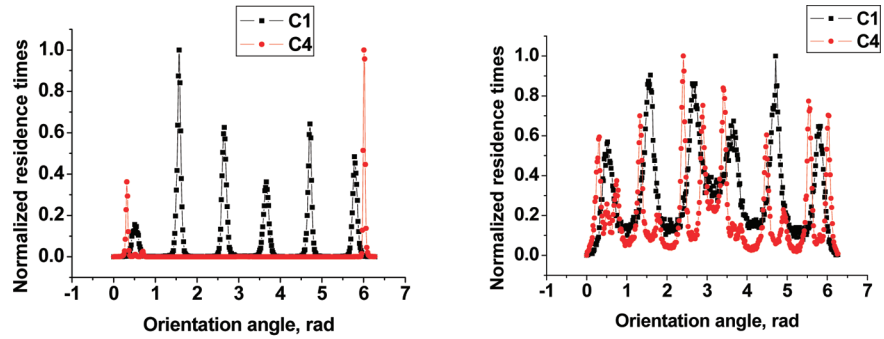

Figure 3. Temperature dependence of rotation dynamics of thioethers. Plots are shown for the distributions of orientation angles for C_1 and C_4 molecules. (a) $T = 25$ K. (b) $T = 100$ K.

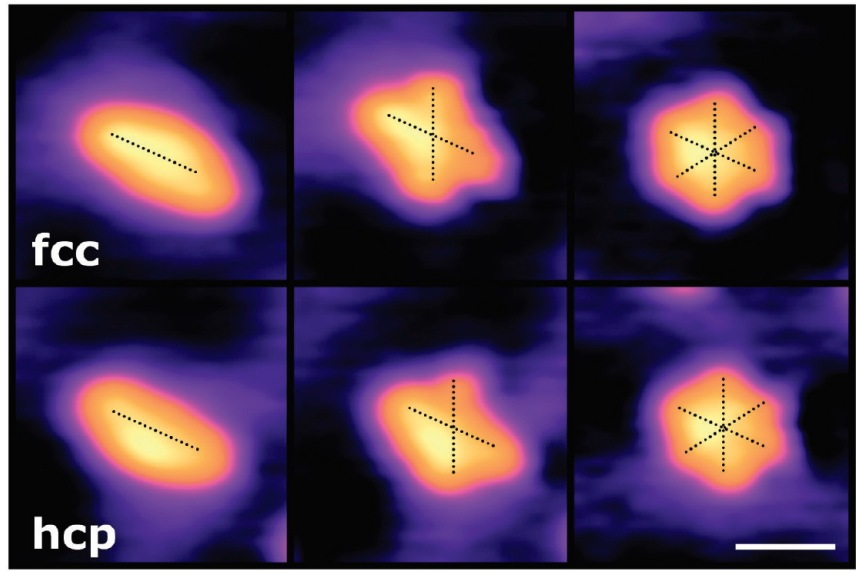

Figure 4. STM images reveal that as dibutyl sulfide (C_4) molecules bound to both fcc and hcp areas of the Au(111) surface are heated, their appearance changes from linear to rectangular to hexagonal (left to right). These changes in appearance occur as the molecules sample first two then all of the three distinct orientations on the Au surface. ($I = 10$ pA, $V_{tip} = 0.3$ V. T_{linear}, 7 K; $T_{rectangular}$, 13 K; $T_{hexagonal}$, 25 K). Scale bar = 1 nm.

characteristic "herringbone reconstruction"), the 3-fold symmetry is broken slightly. This caused one of the three nearly equivalent orientations of the molecule to lie at a slightly different energy than the other two. This small difference in energy is the reason why the thioether molecules appeared rectangular before they rotated fully and imaged as hexagons (see Figure 4). This intermediate, rectangular state occurred for both diethyl (C_2) and dibutyl (C_4) sulfide molecules at 12 ± 3 K.

The details of how temperature affected the rotational efficiency of dibutyl sulfide (C_4) molecules are presented in Figure 5. At $T = 25$ K, the C_4 molecule was found preferentially in only one orientation because it did not have enough energy to explore other potential minima in the free-energy profile. At $T = 78$ K, the thermal energy was high enough to overcome some of the rotational barriers, and C_4 was found at four possible orientations with similar probabilities. At even higher temperature ($T = 100$ K) the number of preferred orientations increased to six. In addition, the rotational dynamics were similar on fcc and hcp surface domains. These theoretical results nicely reproduce the linear, rectangular, and hexagonal appearance of thioethers rotors as seen in the STM images (see Figure 4).

It should be noted that the number of possible orientations of the rotor is determined by the symmetry of the surface. If only the first layer of the Au(111) surface is taken into account, then only six possible orientations of the molecule should be expected (assuming that one alkyl chain is the head and the other one is the tail). However, due to the presence of the second and the third layers, there are six additional orientations due to two separate types of 3-fold site based on the Au atoms in the second layer. For this system, one of these 3-fold sites is less energetically favorable. In addition, MD runs are limited to several nanoseconds, limiting the possibilities for the exploration of thioethers on the surface. These are the main reasons why more complex orientation probabilities were observed with smaller peaks at higher temperatures, as shown in Figure 5.

Quantitative analysis of MD trajectories allowed the rotational frequencies of thioethers to be measured. The results for the rotational activation energies are presented in Figure 6. Similar to experimental observations, computer simulations predicted a jump in rotational barriers when going from C_1 to C_2 molecules; however, the activation energies were almost constant or very slowly increased for larger thioethers ($n > 2$), although this depended on the surface domain. Experiments showed almost unhindered rotations of the C_1 molecules with a barrier of less than 0.5 kJ/mol,[41] while MD calculations gave an activation energy closer to 1 kJ/mol. For C_4, the agreement between the theory and experiments was better; STM measured

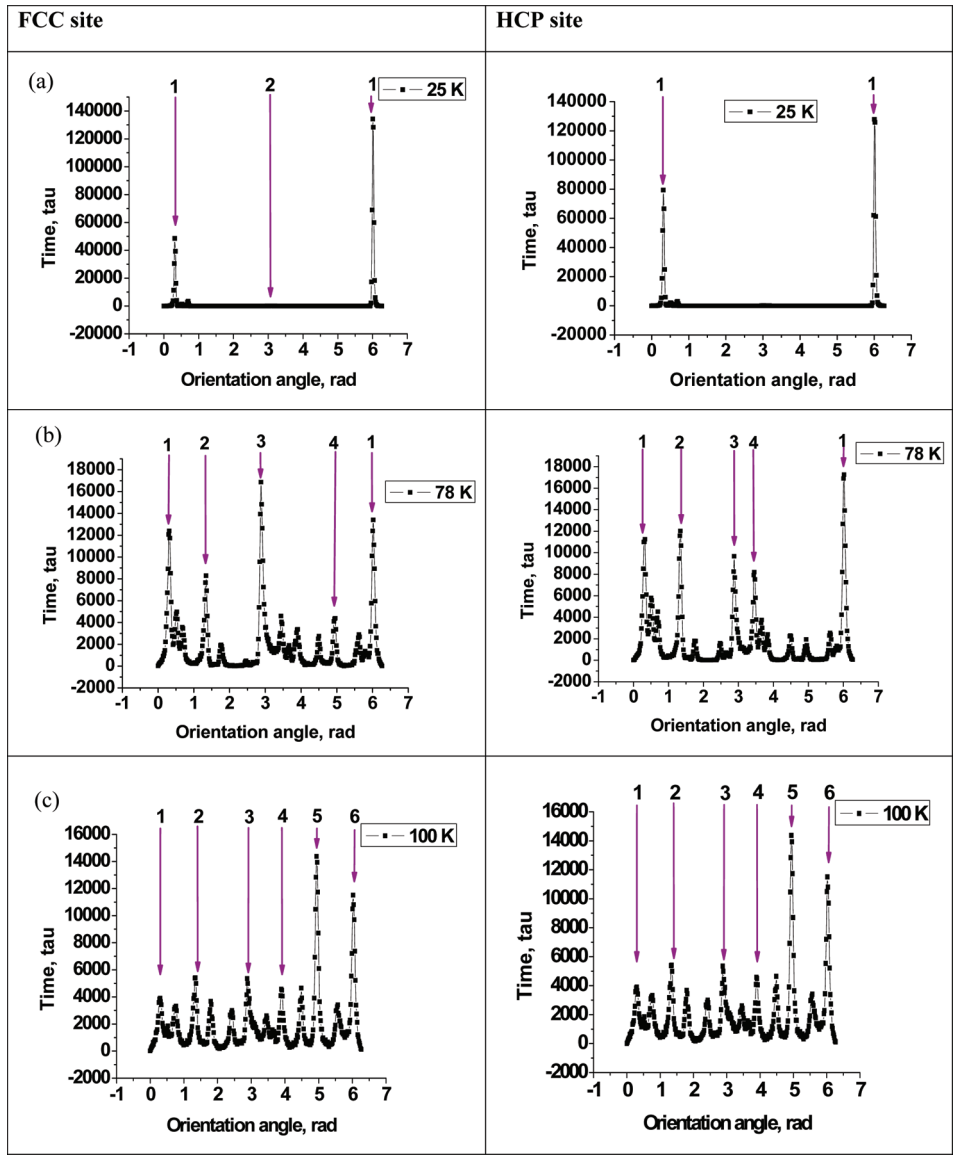

Figure 5. Rotational dynamics of dibutyl sulfide (C_4) on fcc and hcp lattice sites at different temperatures. Plots are shown for the distributions of orientation angles. (a) $T = 25$ K; (b) $T = 78$ K; (c) $T = 100$ K.

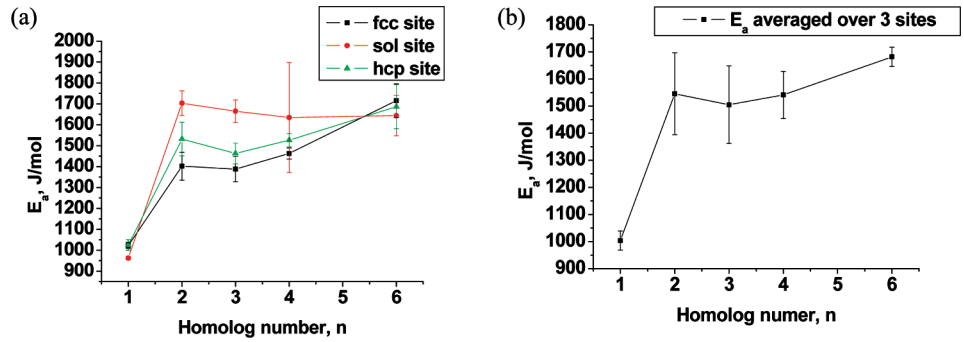

Figure 6. Activation energies for surface rotation of the thioethers as a function of the number of carbon atoms in alkyl chains. (a) Activation energies for three distinct surface sites: fcc, hcp, and soliton (sol). (b) Activation energies averaged over different surface sites.

the barrier at about 1.2 kJ/mol,[41] and theoretical computations yielded ~1.5 kJ/mol.

The observation that rotational barriers were almost independent of the alkyl chain length for C_n molecules (for n larger than 2) is counterintuitive since one could argue that for larger side chains, the number of interactions with the gold surface increases and the rotational activation energies would continue to increase sharply as a function of n. These predicted trends were not observed experimentally. The alkyl side chains of thioethers were rather flexible and as a result, in most of their molecular conformations, only part of the molecule was in contact with the surface. Thus, there are at least two factors that defined the rotational activation energies. Increasing the length of the alkyl chain led to stronger interactions with the

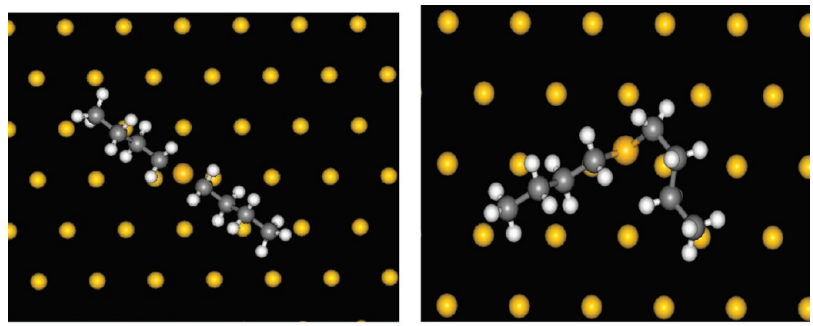

Figure 7. Structures of the dibutyl sulfide molecule (C_4) with artificially frozen degrees of freedom. (a) Fully frozen, 1 linear rigid group; (b) Partially frozen, 3 rigid groups: 2 alkyl chains and a sulfur atom.

TABLE 1: Activation Energies for Dibutyl Sulfide (C_4) Molecules with Different Degrees of Allowed Internal Motions

type of freezing	activation energy, E_a, J/mol
fully flexible molecule = 9 rigid groups	1214.06
frozen alkyl chains = 3 rigid groups	1202.58
frozen molecule = 1 rigid group	2754.55

surface (due to the larger number of atoms interacting with the surface) and slowed down the molecular rotations (i.e., raised the torsional barrier). However, larger alkyl chains were more likely to fold, which decreased the number of atoms that interacted with the surface, and this significantly lowered the activation barriers.

To test this idea, MD computer simulations were run for molecular rotors with some artificially constrained degrees of freedom. The theoretical method presented here is based on the description of any molecule as a collection of coupled rigid-body segments, and the motion of these segments is assumed to be independent from each other. In these MD calculations, the C_n molecules were viewed as consisting of $(2n + 1)$ rigid segments. To freeze some internal dynamics in the molecules, the number of rigid segments was decreased. For example, a fully frozen molecular rotor was made of a single linear rigid segment. Structures of fully frozen and partially frozen C_4 molecules are illustrated in Figure 7. The results for the rotational barriers of C_4 molecules with different internal degrees of freedom are presented in Table 1. Full freezing of the molecular motion led to a significant increase in the activation energies, which was expected from the theoretical predictions. However, partial freezing of alkyl chains did not change the rotational barrier very much. This can be understood if one imagines that the rigid alkyl chains in this artificial molecule were free to move around the sulfur atom in any direction. There were also many molecular conformations where the chains were not close to the gold surface, and this lowered the effective interaction. The rotational properties for different thioethers were also calculated with frozen degrees of freedom and then compared to the fully flexible, realistic molecules. Figure 8 shows that molecules with frozen degrees of freedom should rotate slower. This observation supports the idea that folding dynamics of alkyl chains is one of the factors responsible for lowering the effective rotational barriers in thioethers.

Although the theoretical prediction that the flexibility of alkyl chains lowers the activation energies agrees well with both experimental observations and MD computer simulations, it still cannot explain the effective saturation for rotational barriers as functions of alkyl chain lengths. Figure 8 shows that even for

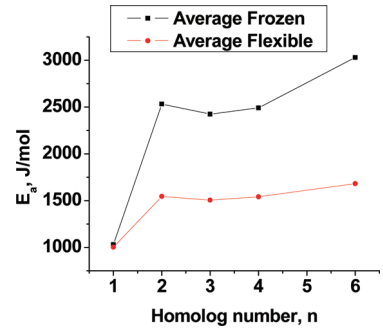

Figure 8. Activation energies for surface rotations (averaged over distinct lattice sites) for fully flexible and rigid C_n molecules.

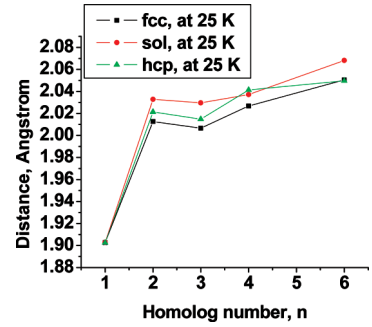

Figure 9. Distances between the sulfur atom and the gold surface for different thioethers on distinct lattice sites at $T = 25$ K.

rigid molecules the saturation regime is observed, although to less of a degree and for significantly larger rotational energies. It is proposed that this phenomenon is due to increased steric repulsion between thioether molecules and the Au(111) surface that lowers the effective interactions with the surface. To check this idea, the average distance between the sulfur atom and the gold surface was plotted for different dialkyl sulfides (see Figure 9). This distance jumps when n changes from 1 to 2, but then increases rather slowly for distinct lattice sites. It can be argued that increasing the size of alkyl chains increases the number of atoms that can interact with the surface, but it also leads to larger steric repulsions between the thioether molecule and the gold surface. This effect is responsible for saturation regime in activation energies for rotation. It seems from experimental measurements and from MD computer simulations that these factors almost cancel each other out for larger C_n molecules leading to a plateau in the torsional barrier above C_2. These results also suggest that the rotational dynamics of thioethers can be controlled and modified by chemically altering the flexibility, chemical composition and steric interactions of the side chains with the surface.

Experimentally observed and computed rotational barriers for thioethers are rather small, suggesting that the approximations used in MD simulations and the details of the force field might have a considerable effect on theoretical estimates. For example, it was assumed that the surface atoms are frozen, and it is not clear how important the mobility of the surface gold atoms is for explaining the dynamic properties of the system. One could argue that because all of the measurements and calculations have been done at low temperatures, and the only strong interactions in the systems are between the sulfur and gold atoms, the effect of surface atom mobility is probably negligible. In addition, the theoretical results are concerned mostly with the explanation of trends rather than specific values of rotational properties. However, future calculations will investigate the rotational dynamics of thioethers by utilizing MD simulations with different force fields and with more realistic descriptions of the system.

4. Conclusions

This study presented a comprehensive experimental and theoretical investigation of molecular rotations of symmetric thioethers on gold surfaces. Measuring the rotational dynamics of single molecules at different temperatures using STM revealed that the activation barrier was almost constant for dialkyl sulfides with different alkyl chain lengths, with the exception of the shortest (dimethyl sulfide) which rotated significantly faster. These results seem to contradict the naïve expectations that increasing the number of atoms should increase the effective interactions with the surface and slow the rotational dynamics. To resolve the mechanism of the unusual rotational dynamics of thioethers, rigid-body molecular dynamics simulations were performed. These theoretical calculations for the rotational properties of dialkyl sulfides were in good agreement with observed experimental properties. To explain this observed behavior, a hypothesis was proposed that rotational dynamics is determined by two factors: the length of alkyl chains and the flexibility of the molecules. Because the side chains were flexible, the effective number of atoms that strongly interacted with the surface was rather small, and the rotations were not hindered significantly by increasing the length of the alkyl segments. MD simulations were also performed for molecular rotors with frozen folding dynamics, and these calculations showed a significant increase in the rotational barriers, which agreed with theoretical predictions. However, the flexibility alone could not explain the observed saturation regime in rotational energies for larger thioethers. This phenomenon was explained by analyzing MD computer simulations that showed increased steric repulsion with the surface that effectively canceled the increasing interactions. Thus a combination of experimental and theoretical methods allowed us to uncover the complex mechanisms of molecular rotations in dialkyl sulfides on gold surfaces.

These experimental and theoretical investigations indicate that gold-supported thioether molecular rotors are a convenient and robust system for studying molecular rotation at the single-molecule level. To understand general mechanisms of rotational motion, it will be important in future work to investigate asymmetric rotors, dipolar rotors and molecules with different groups that strongly interact with the surface. We suggest that the approach presented here, which combines theoretical and experimental methods, is a powerful tool for analyzing and understanding such complex systems at the nanoscale.

Acknowledgment. A.B.K. would like to acknowledge the support from the Welch Foundation (Grant C-1559) and from the U.S. National Science Foundation (Grant ECCS-0708765). A.E.B. and H.L.T. thank the U.S. Department of Education for GAANN fellowships. E.C.H.S. acknowledges support from NSF (CHE-0844343), Research Corporation, and the Beckman Foundation.

Supporting Information Available: This material is available free of charge via the Internet at http://pubs.acs.org.

References and Notes

(1) Lodish, H.; Zipursky, S. L.; Matsudaira, P.; Baltimore, D.; Darnell, J. *Molecular Cell Biology*, 4th ed.; W.H. Freeman and Company: New York, 2000.
(2) Bray, D. *Cell Movements: from molecules to motility*, 2nd ed.; Garland Publishing: New York, 2001.
(3) Howard, J. *Mechanics of Motor Proteins and the Cytoskeleton*; Sinauer Associates: Sunderland, MA, 2001.
(4) Schliwa, M.; Woehlke, G. *Nature (London)* **2003**, *422*, 759.
(5) Kolomeisky, A.; Fisher, M. E. *Annu. Rev. Phys. Chem.* **2007**, *58*, 675.
(6) Shirai, Y.; Morin, J.-F.; Sasaki, T.; Guerrero, G. M.; Tour, J. M. *Chem. Soc. Rev.* **2006**, *35*, 1043.
(7) Van Delden, R. A.; ter Wiel, M. K. J.; Pollard, M. M.; Vicario, J.; Koumura, N.; Feringa, B. L. *Nature (London)* **2005**, *437*, 1337.
(8) Kelly, T. R.; Silva, R. A.; De Silva, H.; Jasmin, S.; Zhao, Y. *J. Am. Chem. Soc.* **2000**, *122*, 6935.
(9) Leigh, D. A.; Wong, J. K. Y.; Dehez, F.; Zerbetto, F. *Nature (London)* **2003**, *424*, 174.
(10) Hernandez, J. V.; Kay, E. R.; Leigh, D. A. *Science* **2004**, *306*, 1532.
(11) Koumura, N.; Zijlstra, R. W.; van Delden, R. A.; Harada, N.; Feringa, B. L. *Nature (London)* **1999**, *401*, 152.
(12) Alvey, M. D.; Yates, J. T., Jr.; Uram, K. J. *J. Chem. Phys.* **1987**, *87*, 7221.
(13) Stipe, B. C.; Rezaei, M. A.; Ho, W. *Science* **1998**, *279*, 1907.
(14) Horinek, D.; Michl, J. *Proc. Natl. Acad. Sci. U.S.A.* **2005**, *102*, 14175.
(15) Fendrich, M.; Wagner, Th.; Stohr, M.; Moller, R. *Phys. Rev. B* **2006**, *73*, 115433.
(16) Hou, S.; Sagara, T.; Xu, D.; Kelly, T. R.; Ganz, E. *Nanotechnology* **2003**, *14*, 566.
(17) Gimzewski, J. K.; Joachim, C.; Schlittler, R. R.; Langlais, V.; Tang, H.; Johannsen, I. *Science* **1998**, *281*, 531.
(18) Magnera, T. F.; Michl, J. *Top. Curr. Chem.* **2005**, *262*, 63.
(19) Stohr, M.; Wagner, T.; Gabriel, M.; Weyers, B.; Moller, R. *Phys. Rev. B* **2002**, *65*, 33404.
(20) Wahl, M.; Stohr, M.; Spillmann, H.; Jung, T. A.; Gade, L. H. *Chem. Commun.* **2007**, 1349.
(21) Wintjes, N.; Bonifazi, D.; Cheng, F. Y.; Kiebele, A.; Stohr, M.; Jung, T.; Spillmann, H.; Diederich, F. *Angew. Chem., Int. Ed.* **2007**, *46*, 4089.
(22) Vaughan, O. P. H.; Williams, F. J.; Bampos, N.; Lambert, R. M. *Chem. Int. Ed.* **2006**, *45*, 3779.
(23) Ye, T.; Takami, T.; Wang, R. M.; Jiang, J. Z.; Weiss, P. S. *J. Am. Chem. Soc.* **2006**, *128*, 10984.
(24) Takami, T.; Yet, T.; Arnold, D. P.; Sugiura, K.; Wang, R. M.; Jiang, J. Z.; Weiss, P. S. *J. Phys. Chem. C* **2007**, *111*, 2077.
(25) Hersam, M. C.; Guisinger, N. P.; Lyding, J. W. *J. Vac. Sci. Technol., A* **2000**, *18*, 1347.
(26) Stipe, B. C.; Rezaei, M. A.; Ho, W. *Science* **1998**, *279*, 1907.
(27) Dunphy, J. C.; Rose, M.; Behler, S.; Ogletree, D. F.; Salmeron, M.; Sautet, P. *Phys. Rev. B* **1998**, *81*, 1263.
(28) Matsumoto, C.; Kim, Y.; Okawa, T.; Sainoo, Y.; Kawai, M. *Surf. Sci.* **2005**, *587*, 19.
(29) Sainoo, Y.; Kim, Y.; Okawa, T.; Komeda, T.; Shigekawa, H.; Kawai, M. *Phys. Rev. Lett.* **2005**, *95*, 246102.
(30) Sainoo, Y.; Kim, Y.; Komeda, T.; Kawai, M.; Shigekawa, H. *Surf. Sci.* **2003**, *536*, L403.
(31) Kottas, G. S.; Clarke, L. I.; Horinek, D.; Michl, J. *Chem. Rev.* **2005**, *105*, 1281.
(32) Clarke, L. I.; Horinek, D.; Kottas, G. S.; Varaksa, N.; Magnera, T. F.; Hinderer, T. P.; Horansky, R. D.; Michl, J.; Price, J. C. *Nanotechnology* **2002**, *13*, 533.
(33) Wang, B.; Zheng, X. L.; Michl, J.; Foley, E. T.; Hersam, M. C.; Bilic, A.; Crossley, M. J.; Reimers, J. R.; Hush, N. C. *Nanotechnology* **2004**, *15*, 324.
(34) Zheng, X. L.; Mulcahy, M. E.; Horinek, D.; Galeotti, F.; Magnera, T. F.; Michl, J. *J. Am. Chem. Soc.* **2004**, *126*, 4540.

(35) Rao, B. V.; Kwon, K. Y.; Liu, A. W.; Bartels, L. *J. Chem. Phys.* **2003**, *119*, 10879.
(36) Rao, B. V.; Kwon, K. Y.; Liu, A. W.; Bartels, L. *Proc. Natl. Acad. Sci. U.S.A.* **2004**, *101*, 17920.
(37) Vacek, J.; Michl, J. *Adv. Funct. Mater.* **2007**, *17*, 730.
(38) Horinek, D.; Michl, J. *J. Am. Chem. Soc.* **2003**, *125*, 11900.
(39) Horinek, D.; Michl, J. *Proc. Natl. Acad. Sci. U.S.A.* **2005**, *102*, 14175.
(40) Maksymovych, P.; Sorescu, D. C.; Dougherty, D.; Yates, J. T. *J. Phys. Chem. B* **2005**, *109*, 22463.
(41) Baber, A. E.; Tierney, H. L.; Sykes, E. C. H. *ACS Nano* **2008**, *2*, 2385.
(42) Akimov, A. V.; Nemukhin, A. V.; Moskovsky, A. A.; Kolomeisky, A. B.; Tour, J. M. *J. Chem. Theory Comput.* **2008**, *4*, 652.
(43) Okumura, H.; Itoh, S. G.; Okamoto, Y. *J. Chem. Phys.* **2007**, *126*, 084103.
(44) Dullweber, A.; Leimkuhler, B.; McLahlan, R. *J. Chem. Phys.* **1997**, *107*, 5840.
(45) Rappe, A. K.; Casewit, C. J.; Colwell, K. S.; Goddard III, W. A.; Skiff, W. M. *J. Am. Chem. Soc.* **1992**, *114*, 10024.
(46) Mahaffy, R.; Bhatia, R.; Garrison, B. J. *J. Phys. Chem. B* **1997**, *101*, 771.
(47) Barth, J. V.; Brune, H.; Ertl, G.; Behm, R. J. *Phys. Rev. B* **1990**, *42*, 9307–9318.
(48) Woll, C.; Chiang, S.; Wilson, R. J.; Lippel, P. H. *Phys. Rev. B* **1989**, *39*, 7988–7991.

JP9017844